

Available online at [www.sciencedirect.com](http://www.sciencedirect.com)

Biochimica et Biophysica Acta 1773 (2007) 1786–1792

[www.elsevier.com/locate/bbamcr](http://www.elsevier.com/locate/bbamcr)

# Identification of PatL1, a human homolog to yeast P body component Pat1

Nicoletta Scheller<sup>a,1</sup>, Patricia Resa-Infante<sup>b,1,2</sup>, Susana de la Luna<sup>b,c</sup>, Rui Pedro Galao<sup>b</sup>,  
Mario Albrecht<sup>d</sup>, Lars Kaestner<sup>e</sup>, Peter Lipp<sup>e</sup>, Thomas Lengauer<sup>d</sup>,  
Andreas Meyerhans<sup>a</sup>, Juana Díez<sup>a,b,\*</sup>

<sup>a</sup> Institute of Virology, Saarland University, 66421 Homburg, Germany

<sup>b</sup> Department of Experimental and Health Sciences, Universitat Pompeu Fabra, 08003 Barcelona, Spain

<sup>c</sup> ICREA and Genes and Disease Program, Centre de Regulació Genòmica-CRG 08003 Barcelona, Spain

<sup>d</sup> Max Planck Institute for Informatics, Stuhlsatzenhausweg 85, 66123 Saarbrücken, Germany

<sup>e</sup> Institute for Molecular Cell Biology, Saarland University, 66421 Homburg, Germany

Received 17 April 2007; received in revised form 23 August 2007; accepted 24 August 2007

Available online 6 September 2007

## Abstract

In yeast, the activators of mRNA decapping, Pat1, Lsm1 and Dhh1, accumulate in processing bodies (P bodies) together with other proteins of the 5'-3'-deadenylation-dependent mRNA decay pathway. The Pat1 protein is of particular interest because it functions in the opposing processes of mRNA translation and mRNA degradation, thus suggesting an important regulatory role. In contrast to other components of this mRNA decay pathway, the human homolog of the yeast Pat1 protein was unknown. Here we describe the identification of two human *PATL1* genes and show that one of them, *PATL1*, codes for an ORF with similar features as the yeast PAT1. As expected for a protein with a fundamental role in translation control, *PATL1* mRNA was ubiquitously expressed in all human tissues as were the mRNAs of LSM1 and RCK, the human homologs of yeast LSM1 and DHH1, respectively. Furthermore, fluorescence-tagged PatL1 protein accumulated in distinct foci that correspond to P bodies, as they co-localized with the P body components Lsm1, Rck/p54 and the decapping enzyme Dcp1. In addition, as for its yeast counterpart, PatL1 expression was required for P body formation. Taken together, these data emphasize the conservation of important P body components from yeast to human cells.

© 2007 Elsevier B.V. All rights reserved.

**Keywords:** Pat1; Decapping; mRNA turnover; Processing bodies; P bodies

## 1. Introduction

Distinct cytoplasmic foci named processing bodies (P bodies) have recently emerged as dynamic compartments with key roles in the regulation of cellular mRNA fates. P bodies are conserved from yeast to humans and are sites where mRNAs that are not translated are directed either to the degradation or to storage for subsequent return to translation [1–5]. Consistent with this role, translationally inactive mRNAs co-localize in P bodies together with proteins that function in translation repression, mRNA-

mediated silencing, mRNA surveillance and mRNA degradation [1–5].

A conserved core of proteins from the mRNA decay machinery is found in P bodies from yeast to humans, however, it is important to note that there is an increased complexity in P body composition and function in higher eukaryotes [2,3,5]. Thus, human P bodies contain additional proteins that have no yeast counterparts, for example, factors involved in RNAi such as GW182 or Argonaute proteins. Moreover, in *Saccharomyces cerevisiae* P bodies increased in size and number by exposing yeast cells to growth limitation, increased cell density or stress [6] while in humans, P body's size and numbers are increased in proliferating cells [7].

From the two main eukaryotic pathways of mRNA decay, the 3'-5'-deadenylation-dependent exonucleolytic pathway and the 5'-3'-deadenylation-dependent decapping pathway, only the proteins required for the latter have yet been shown to localize in

\* Corresponding author. Departamento Ciencias Experimentales y de la Salud, Universitat Pompeu Fabra, PRBB, Dr. Aiguader 88, 08003, Barcelona, Spain. Tel.: +34 93 3160 862; fax: +34 93 3160 901.

E-mail address: [juana.diez@upf.edu](mailto:juana.diez@upf.edu) (J. Díez).

<sup>1</sup> These authors contributed equally to this work.

<sup>2</sup> Present address: Centro Nacional de Biotecnología (CSIC), Darwin 3, Cantoblanco, 28049 Madrid, Spain.

P bodies. In yeast, these include the decapping enzyme Dcp1/Dcp2, the 5'-to 3'-exonuclease Xrn1 and proteins that function as activators of decapping such as the helicase Dhh1, the heteroheptameric Lsm1–7 ring and Pat1 [8]. The mechanisms by which these proteins promote decapping are unknown, however, they directly interact and form a complex [8–11]. Interestingly, under certain conditions such as overexpression and stress, Dhh1 and Pat1 proteins are also required for repression of translation [12].

The yeast Pat1 protein has very interesting features. In addition to its role in translation repression and mRNA degradation mentioned above, it is also required for translation initiation [13]. Furthermore, Pat1 is the only decapping activator protein that, besides interacting with deadenylated mRNAs, also binds to eIF4G-, eIF4E- and Pab1p-associated polyadenylated mRNA and locates to polysomes [9,14]. The function of Pat1 in the antagonistic processes of translation and translation repression/mRNA degradation suggest a key regulatory role for this protein. In fact, since the exit of the mRNA from translation to a non-translation state seems crucial for P body formation and Pat1 is associated to the mRNA in both states, it has been suggested that Pat1 could act as a seed protein for P body formation [8].

The 5'-3'-deadenylation-dependent decapping pathway of mRNA degradation is well conserved from yeast to humans. With the exception of Pat1, all the corresponding human homologs have been identified and shown to localize in P bodies as do their yeast counterparts ([2] and references therein). The only characterized homolog of Pat1 in higher eukaryotes was identified in early stage oocytes of *Xenopus* [15]. The protein, named p100, locates to the cytoplasm [15] and co-precipitates with non-adenylated and polyadenylated mRNA [16]. These similarities to its yeast counterpart suggest that Pat1 function is conserved in higher eukaryotes. Here we describe the human homologs of the yeast Pat1 protein and show that one of them, PatL1, is located in P bodies and required for their formation.

## 2. Materials and methods

### 2.1. In silico protein sequence analysis

We retrieved PatL1-related protein sequences and ESTs from the Ensembl (<http://www.ensembl.org>) and NCBI (<http://www.ncbi.nlm.nih.gov>) databases [17,18] using BLAST-based sequence searches [19] for homologs of *S. cerevisiae* Pat1 (YCR077C). The multiple sequence alignment of the identified PatL1 homologs was generated with the program MAFFT [20] (Fig. S3) and the human PatL1 and PatL2 sequence alignment by CLUSTAL W [21] (Fig. S4). The alignment figures were prepared and illustrated using the editor Jalview [22]. We used the online service PSIPRED [23] to predict the secondary structure of PatL1 homologs in five different species (Fig. S3); some divergence of the predicted structures is expected because of prediction inaccuracies and relatively low sequence conservation between species.

### 2.2. Plasmids

cDNA clones corresponding to PATL1 (RZPD: DKFZp4511053) and PATL2 (IMAGE: 5227850) sequences were purchased from Deutsches Ressourcenzentrum fuer Genomforschung (<http://www.rzpd.de>). For the expression of fluorescence-tagged PatL1 in mammalian cells, the PATL1 ORF was amplified by PCR with specific primers introducing a 5'-*Xho*I site followed by a Kozak

consensus site [24] and a 3'-*Xma*I site that results in a deletion of the stop codon. The corresponding PCR fragment was then subcloned into pDsRed1-N1, pDsRed1-C1, pEGFP-N1 and pEGFP-C1 (BD Clontech) by using the *Xho*I and *Xma*I restriction sites. All the primers used for these and constructs described below are given in the Supplemental materials (Table S2). The GFP-DCP1 plasmid with an EGFP-N1 backbone was previously described [25].

For the generation of <sup>32</sup>P-labeled RNA probes, five pGEMT-derived constructs containing between 400 and 570 nt of the corresponding ORFs were generated by PCR amplification and subsequent ligation into pGEMT vectors (Promega). PATL1 and PATL2 sequences were amplified from the above described cDNA clones, LSM1 and RCK sequences from pYCFPhLSM1 [26] and pQE30/RCK [27], respectively, and β-actin sequence from human genomic DNA. All generated constructs were confirmed by DNA sequence analysis.

### 2.3. Northern and Western blot analysis

The Northern blot membranes containing poly (A)<sup>+</sup> RNA from human adult and fetal tissues were purchased from BD Clontech. For the generation of (–) strand <sup>32</sup>P-labeled RNA probes, the linearized pGEM-T-derived plasmids were used for in vitro transcription with Strip-EZ™ RNA SP6/T7 kit (Ambion). Hybridizations were performed with ULTRAhyb® Ultrasensitive Hybridization Buffer (Ambion). Radioactive signals were visualized and quantified using a Molecular Dynamics Typhoon 8600 Phosphorimager and ImageQuant 5.2 software.

For protein extraction, cells were harvested in ice-cold phosphate-buffered saline, sonicated and centrifuged (10,000×g for 20 min at 4 °C). Western blots were performed following standard procedures [28]. The luminescence signals were visualized and quantified using the FUJIFILM Luminescent image analyzer LAS-100 and the Image Gauge 3.12 program.

### 2.4. Antibodies and small interfering RNAs

The following primary antibodies were used: rabbit anti-Lsm1 polyclonal antibody [26] (1:1000 dilution), rabbit anti-Rck/p54 polyclonal antibody (MBL International Co.) (1:500 and 1:2000 dilutions for Western and immunofluorescence analysis, respectively) and mouse anti-tubulin monoclonal antibody (Sigma) (1:1000 dilution). The following secondary antibodies were used: peroxidase-conjugated goat anti-mouse and anti-rabbit antibodies (Sigma) (1:1000 dilution) and Alexa568-conjugated goat anti-rabbit antibody (Molecular Probes) (1:2000 dilution).

Rck/p54 (sense strand: 5'-GGAGGAGAGCAUCCCAUUTT-3'), PatL1 #1 (sense strand: 5'-CUAGAAGAUCAGCUAUUATT-3') and PatL1 #2 (sense strand: 5'-CCAGGAAGUCUGAAUACCATT-3') siRNA duplexes were purchased from Ambion. The siControl Non-targeting siRNA #1 (Dharmacon) was used as a negative control.

### 2.5. Cell culture, transfection and FACS analysis

HeLa cells were grown as recommended by the American Type Cell Culture Collection. Transfections were performed on glass slides (Menzel Gläser) after cells had reached 60% confluency by using LipofectAMIN™2000 (Invitrogen). Cells were processed 24 to 30 h post-transfection with marker plasmids and 72 h post-transfection with siRNAs. All siRNAs were transfected at a final concentration of 50 nM. FACS analysis of 2×10<sup>4</sup> cells were performed between wavelengths of 515 to 545 nm in a FACScan (Becton Dickinson) using CellQuest™ Version Mac App<sup>R</sup> 3.0.1.

### 2.6. Immunofluorescence and co-localization analysis

Immunofluorescence analysis were performed as previously described [26]. The cells were mounted in Vectashield mounting medium with DAPI (Vector Laboratories, Inc.). Images were visualized using a LeitzAristoplan fluorescence microscope. The digitized images were taken with a AxioCamColor camera (Zeiss) and analysed with AxioVision 3.0 programme (Zeiss). The pictures were then compiled with Adobe Photoshop® 5.0.

Confocal imaging was performed using a Nipkow-disc-based scanning head (QLC-100, VisiTech international) attached to an upright microscope (Eclipse 600, Nikon) equipped with a 100× oil lens (Plan Apo 1.4, Nikon). The light

sources were a 488-nm and 561-nm solid-state laser (Sapphire 488-30, Coherent and YCA-series, Melles Griot, respectively). A double-dichroic mirror between the microlens- and pinhole-disc reflects the emission light in the range between 500 and 550 nm as well as above 580 nm. Background light was eliminated using appropriate barrier filter. To check for co-localization, images were analyzed using ImageJ software (Wayne Rasband, National Institute of Mental Health).

### 3. Results and discussion

#### 3.1. Sequence homology of human *PatL1* and *PatL2* to yeast *Pat1*

To identify the human homolog of the *S. cerevisiae* *Pat1* protein, a PSI-BLAST search was performed using the amino acid sequence of *Pat1* as query. Two human ENSEMBL entries with significant homology were found, indicating the existence of two different *Pat1* homologs in humans. The corresponding genes ENSG00000166889 and ENSG00000184710 were named *PAT1*-like 1 (*PATL1*) and *PAT1*-like 2 (*PATL2*), respectively. *PATL1* maps to 11q12.1, consists of at least 18 exons and encodes one predicted open reading frame (ORF) of 770 amino acids (Figs. S1, S4). *PATL2* maps to 15q21.1 and consists of at least 15 exons. The comparison of different cDNA sequences from *PATL2* indicates that several alternative splicing events may take place (Figs. S2, S4).

Based on current gene databases, the existence of two *PAT1* homologs is also observed in other vertebrates, while invertebrates have only a single *PAT1* gene (Table S1). When compiling a multiple protein sequence alignment of the ENSEMBL sequences of *PatL1* and *PatL2* homologs, including yeast *Pat1*, *Patr1* from *Caenorhaditis elegans* and CG5208 from *Drosophila melanogaster* [2] (Fig. S3, Table S1), we found that the highest level of homology lies within the C-terminal part of *PatL1*- and *PatL2*-related proteins. Interestingly, twelve amino acids are strictly conserved in all *Pat1* homologs, suggesting an important functional or structural role. The N-terminal part of the *PatL1* protein, conserved in all *PatL1* homologs but absent in all *PatL2* ones, is rich in aspartates/glutamates and many prolines. A glutamine-rich region and frequently occurring short glutamine-containing sequence motifs (QQ, QxQ and QxxQ) are also contained in human *PatL1* and *PatL2*, which may play a functional role in RNA binding.

#### 3.2. The mRNAs of *PATL1*, *RCK* and *LSM1* are ubiquitously expressed

In yeast, decapping in the main 5'-3'-deadenylation-dependent pathway of mRNA decay is activated by *Pat1*, *Lsm1*–7 and *Dhh1*, which interact with each other in an mRNA-independent manner [9,29–31]. Since this decay pathway is conserved in human cells and is a major player in the regulation of mRNA turnover, one would expect that the human homolog of *Pat1* as well as *Lsm1* and *Dhh1* (named *Rck/p54* in humans) are expressed in all tissues. To test this, we hybridized <sup>32</sup>P-labeled RNA probes derived from the ORFs of human *PATL1*, *PATL2*, *LSM1* and *RCK* genes to poly(A)<sup>+</sup> RNA of various adult human tissues, which was normalized to its  $\beta$ -actin mRNA content in a Northern blot. A main 4.4-kb transcript of *PATL1* was detected in all tissues (Fig. 1). Furthermore, three additional

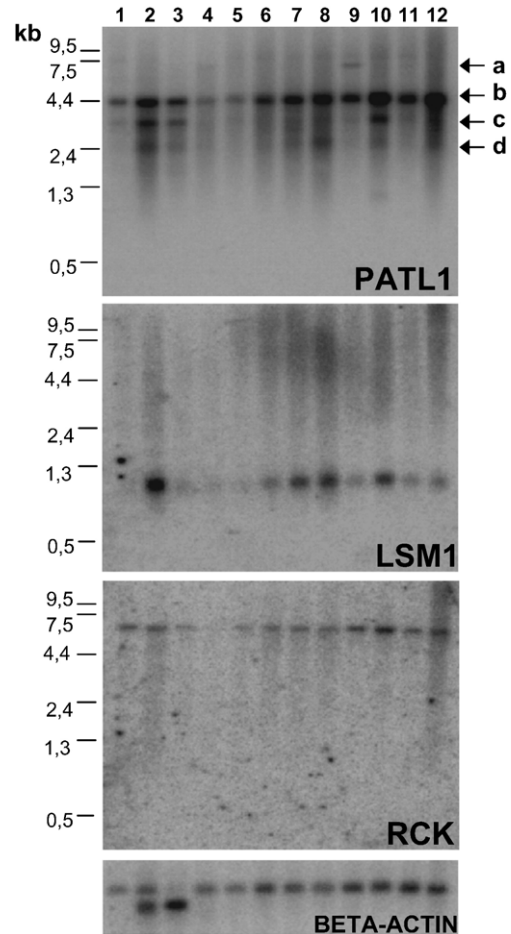


Fig. 1. Northern blot analysis of *PATL1*, *LSM1* and *RCK* mRNAs in various adult human tissues. A Northern blot with poly(A)<sup>+</sup> RNA from adult human brain (lane 1), heart (lane 2), skeletal muscle (lane 3), colon (lane 4), thymus (lane 5), spleen (lane 6), kidney (lane 7), liver (lane 8), small intestine (lane 9), placenta (lane 10), lung (lane 11) and leukocytes (lane 12) was hybridized with <sup>32</sup>P-labeled RNA probes corresponding to *PATL1*, *LSM1* and *RCK* mRNAs. Isoforms of *PATL1* mRNAs are indicated by arrows (a–d). A probe specific for  $\beta$ -actin was used to control equal loading of poly(A)<sup>+</sup> RNA.

transcripts of approximately 7 kb, 3 kb and 2.5 kb were visible with lower intensity in some tissues. Since the *PATL1* gene consists of at least 18 exons, these isoforms could reflect alternative splicing events and/or different sites of polyadenylation. From the four transcripts, only the 4.4 kb and the 3 kb form are supported by cloned cDNAs and are the result of the alternative use of different sites of polyadenylation (Fig. S11). In contrast to *PATL1*, the analysis of *PATL2* expression did not give any detectable signal (data not shown). Since significantly fewer ESTs have been found for *PATL2* than for *PATL1* (more than 200 for *PATL1* vs. 20 for *PATL2*), this would argue that the transcript level of *PATL2* is either very low and/or maybe limited to some specific tissues as is the case of the *Xenopus* ortholog p100 [16].

In addition to *PATL1* transcripts, a *LSM1* transcript of approximately 0.95 kb and a *RCK* transcript of approximately 7.5 kb were detected in all tested tissues (Fig. 1). The transcript sizes were consistent with previously described data (NCBI identifier NM\_014462 and [32]). Interestingly, the mRNA



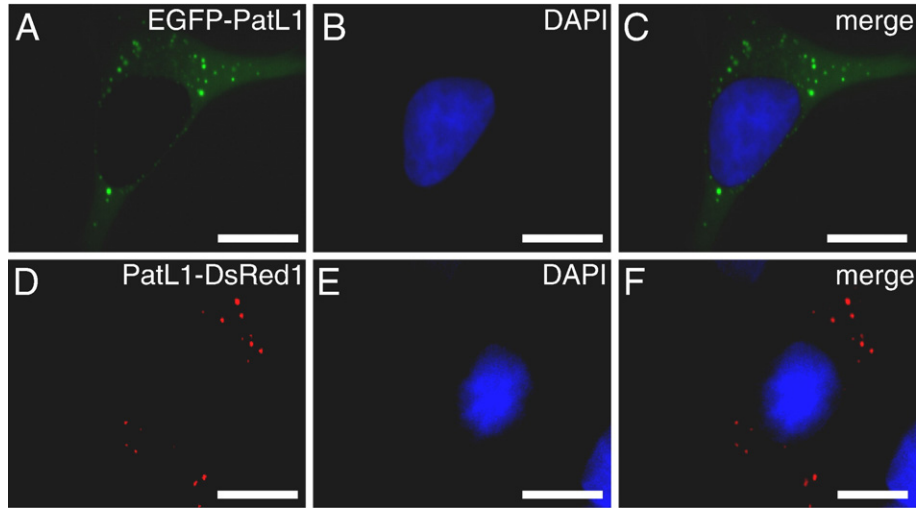


Fig. 2. Fluorescence-tagged PatL1 accumulates in cytoplasmic foci. Transfected HeLa cells expressing either the EGFP fused to the C-terminus of PatL1 (PatL1-EGFP) (A–C), or the RFP fused to the C-terminus of PatL1 (PatL1-dsRed1) (D–F) were grown on slides, fixed 24 h after transfection and counterstained with DAPI. Fluorescent proteins were then visualized by confocal microscopy. The EGFP fluorescence is shown in green (A), the RFP fluorescence in red (D) and the DAPI fluorescence in blue (B, E). Merged pictures are shown in the right handed column (C, F). The indicated bars represent 10 μm.

levels varied in different tissues. For instance, high levels of LSM1, RCK and PATL1 transcripts were detected in the heart, whereas the levels in brain tissue were low or moderate (Fig. 1). Assuming that transcript levels correspond to protein levels, this may reflect a tissue-specific regulation of mRNA turnover.

### 3.3. PatL1 accumulates in cytoplasmic foci

The ubiquitous expression of the PATL1 together with the RCK and LSM1 transcripts makes PatL1 the most likely candidate for the yeast Pat1 homolog. We therefore focussed on

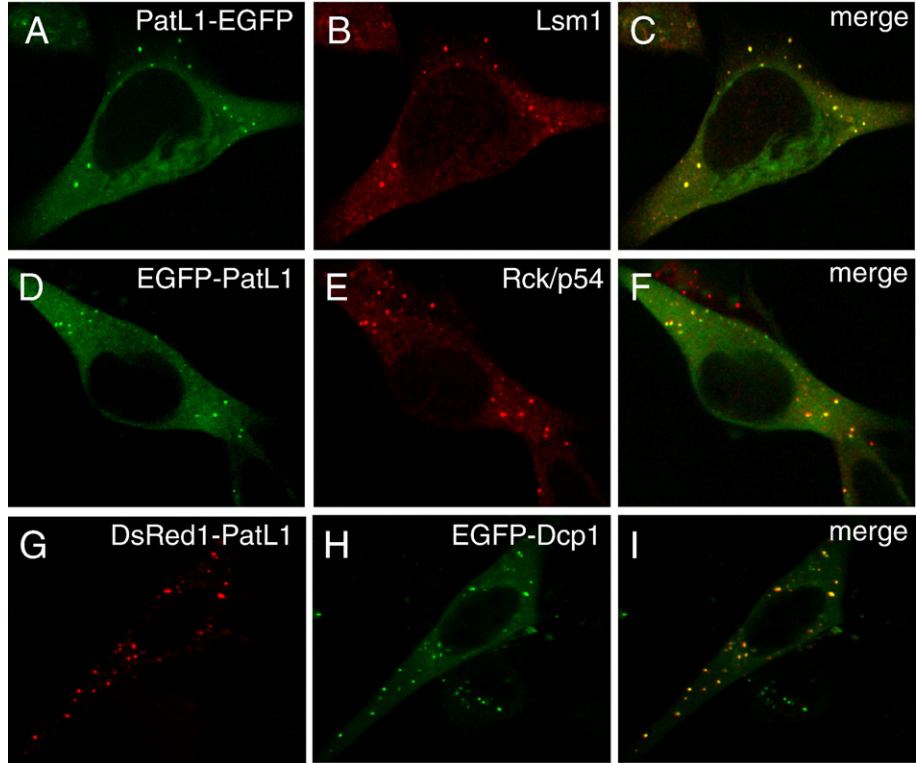


Fig. 3. Co-localization of PatL1 with Lsm1, Rck/p54 and Dcp1 in processing bodies. HeLa cells were transfected with plasmids expressing the EGFP-tag fused to the C-terminus of PatL1 (PatL1-EGFP) (A–C) or to the N-terminus of PatL1 (EGFP-PatL1) (D–F). In addition, the plasmid expressing the RFP-tag fused to the N-terminus of PatL1 (DsRed1-PatL1) was co-transfected with EGFP-Dcp1 (G–I). After transfection, cells were grown for 24 h on slides and fixed. Then, cells were counterstained with anti-Lsm1 antibody (A–C) or anti-Rck/p54 antibody (D–F) and Alexa568-conjugated secondary antibodies. The fluorescence signals were visualized by confocal microscopy. The GFP fluorescence is shown in green (A, D, H), the RFP and Alexa568 fluorescences in red (B, E, G). Merged pictures are shown in the right handed column (C, F, I). The indicated bars represent 10 μm.

this protein in the subsequent studies. To analyze the subcellular distribution of PatL1, plasmids for exogenous expression in mammalian cells of fluorescence-tagged PatL1 were generated. To avoid functional impairment of PatL1 due to its fusion to fluorescent proteins, the fluorescent tags were introduced either at the N- or the C-terminus. In addition, two different fluorescent proteins, the enhanced-green fluorescent protein (EGFP) and the

red fluorescent protein (DsRed1) were used. Western blot analysis of transfected HeLa cells showed that the generated fusion proteins were expressed with the expected molecular weights (data not shown). Then the subcellular localization of the fluorescent proteins was assessed by confocal microscopy in HeLa cells after 24 to 30 h post-transfection of the corresponding plasmids. In contrast to the uniform distribution shown by the

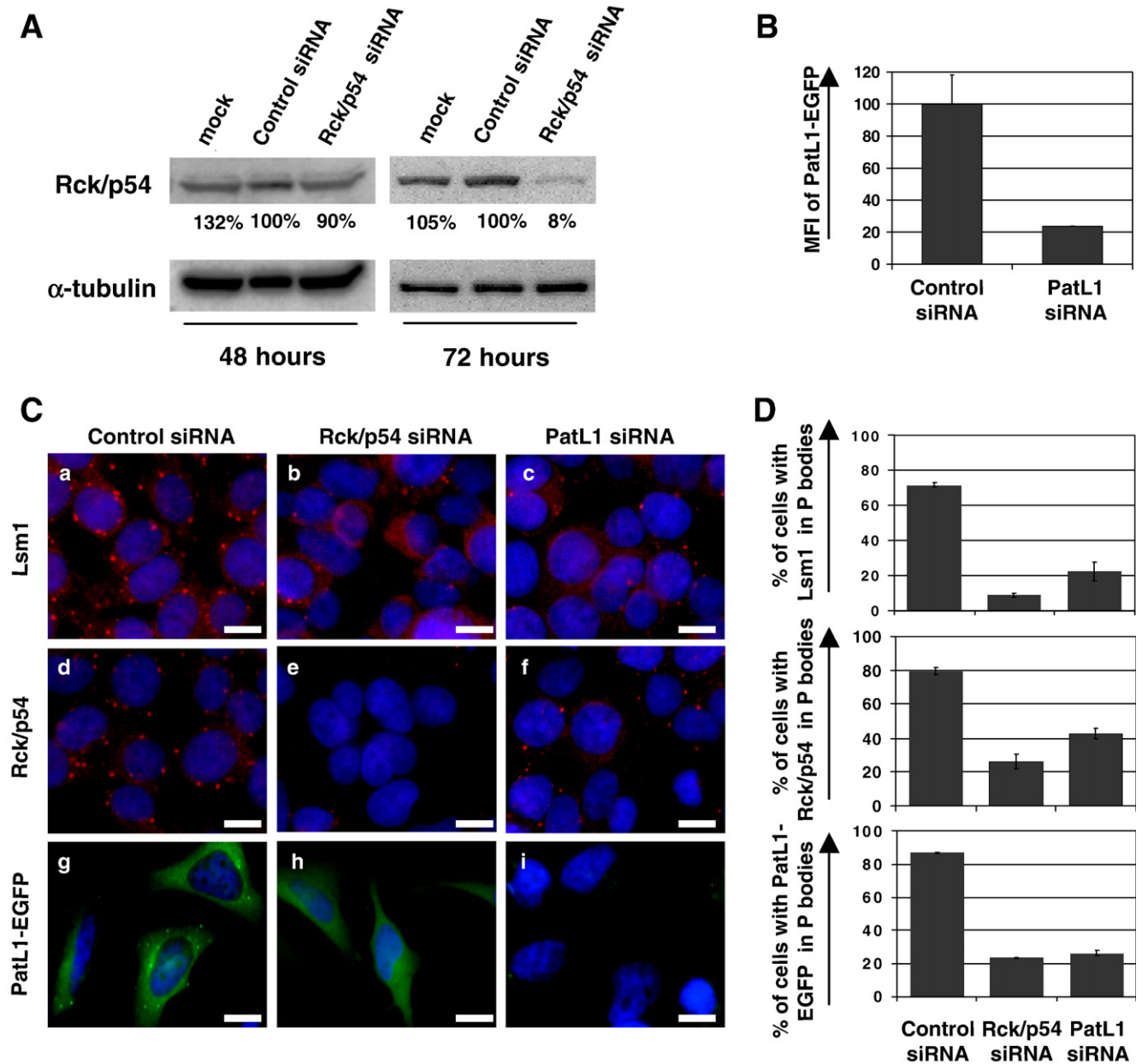


Fig. 4. Reduction of PatL1 or Rck/p54 protein levels leads to P body loss. (A) HeLa cells transfected with either mock, a non-targeting control siRNA or Rck/p54 siRNA were grown for 48 and 72 h. Cells were harvested and protein expression was analyzed by Western blot. The amount of Rck/p54 was normalized to  $\alpha$ -tubulin and set to 100% for non-targeting control siRNA transfection at each time point. (B) HeLa cells transfected either with non-targeting control siRNA or PatL1 siRNA #1 were incubated for 48 h and transfected with PatL1-EGFP. Twenty-four hours later, the cells were analyzed by flow cytometry. The mean fluorescence intensity (MFI) in the FL-1 channel is given on the Y-axis of the graph. (C) HeLa cells transfected either with non-targeting control siRNA (a, d, g), Rck/p54 siRNA (b, e, h) or PatL1 siRNA #1 (c, f, i) were grown for 48 h on slides and were either mock transfected (a–f) or transfected with PatL1-EGFP plasmid (g–i). Twenty-four hours later cells were stained with anti-Lsm1 antibody (a–c), anti-Rck/p54 antibody (d–f) and Alexa568-conjugated secondary antibodies. All cells were counterstained with DAPI (a–i) and visualized by fluorescence microscopy. The EGFP fluorescence is shown in green (g–i), the Alexa568 fluorescence in red (a–f) and the DAPI fluorescence in blue (a–i). The indicated bars represent 10  $\mu$ m. (D) Percentage of cells displaying P bodies visualized by Lsm1, Rck/p54 or PatL1 after silencing of Rck/p54 or PatL1. At least 100 cells per single silencing experiments were counted. Data represent average and S.D. of at least two independent experiments.

fluorescence tags when expressed alone (data not shown), the fluorescence-tagged PatL1 predominantly localized in the cytoplasm in small discrete foci (Fig. 2). Moreover, N-terminally and C-terminally fused PatL1 with either of the fluorescent proteins showed similar localization patterns (Figs. 2 and 3). Thus, the accumulation pattern of PatL1 was specific and independent of the position and the nature of the tag.

### 3.4. PatL1 co-localizes to Lsm1, Rck/p54 and Dcp1 in P bodies

In yeast, Pat1 localizes to P bodies together with other proteins from the 5'-3'-deadenylation-dependent mRNA decay pathway such as Lsm1, Dhh1 and Dcp1, among others [33]. This is also true for all known corresponding human homologs [25,26,34]. To determine whether the localization of the fluorescent-tagged PatL1 in cytoplasmic foci corresponds to P bodies and is not an artefact due to exogenous expression, we tested the co-localization of PatL1 with the well-characterized P body components Rck/p54, Lsm1 and Dcp1. HeLa cells were transfected with a plasmid expressing PatL1 fused to an EGFP or a DsRed1 fluorescence tag. After 24 h, P bodies were visualized with antibodies directed against endogenous Lsm1 and Rck/p54, or by co-expression of EGFP-tagged Dcp1 (Fig. 3). As expected, EGFP-tagged Dcp1, as well as the endogenous Lsm1 and Rck/p54 accumulated in cytoplasmic foci. Importantly, the fluorescent PatL1 signal co-localized to the foci formed by Lsm1, Rck/p54 and Dcp1 fusion protein. This indicates that PatL1, as yeast Pat1, accumulates in P bodies.

### 3.5. PatL1 is required for P body formation

In both, yeast and human cells, depletion of certain P body components influences the size and the number of P bodies. For example, depletion of proteins acting in early stages of the 5'-3'-deadenylation-dependent mRNA decay pathway, such as Dhh1 and its human homolog Rck/p54, leads to a decrease in P body size and number, indicating that these proteins are required for P body formation [12,35]. In contrast, depletion of proteins acting in late stages, such as the exonuclease Xrn1, has the opposite effect [25,33]. To analyze whether PatL1 influences P body formation, we decreased the level of PatL1 in HeLa cells by using siRNAs specific for PatL1. Then we followed the effect of PatL1 depletion on P body formation by visualizing Lsm1, Rck/p54 and PatL1-EGFP localization in P bodies (Fig. 4). As a control, we also included in our analysis siRNAs specific for Rck/p54. Since anti-PatL1-specific antibodies are not available, we followed the silencing activity of the PatL1 siRNAs on the exogenously expressed fluorescent PatL1 by flow cytometry. Seventy-two hours after siRNA transfection of HeLa cells, protein levels of endogenous Rck/p54 and exogenous PatL1-EGFP were decreased by 80% and 92%, respectively (Fig. 4A, B). Based on this kinetics of silencing, cells were transfected either with control siRNA, Rck/p54 siRNA or PatL1 siRNA, grown for 48 h on slides and subsequently mock transfected or transfected with PatL1-EGFP (Fig. 4C). After additional 24 h in culture, cells were fixed and stained with anti-Lsm1 or anti-Rck/p54 for immunofluores-

cence analysis. PatL1 was detected directly via its fluorescent EGFP tag. Silencing of Rck/p54 led to a decrease in the number of P bodies visualized by lack of localization of Rck/p54, Lsm1 and PatL1 in P bodies (Fig. 4C, D). This is consistent with previously described data that show a requirement of Rck/p54 for P body formation in human cells [35,36]. Interestingly, silencing of PatL1 also reduced to a large extent the number of P bodies (Fig. 4C, D) indicating that in human cells PatL1 as Lsm1 and Rck/p54 are required for P body formation. Similar results were obtained with a different PatL1-specific siRNA (data not shown). Thus, human PatL1 parallels yeast Pat1 which when suppressed also leads to P body loss [12,33].

In summary, PatL1 is, together with Lsm1 and Rck/p54, ubiquitously expressed in human tissues, localizes to P bodies and is required for P body formation. These observations strongly support that PatL1 is a human homolog of the yeast Pat1. The conservation of Pat1 from yeast to humans suggests an important role in the regulation of mRNA fates and therefore in translation control. This regulation is crucial in the coordination of cell function both under normal and stressed conditions as, for instance, after virus infections or cell transformation. Indeed, by using a yeast system it has been recently shown that the P body components Pat1, Lsm1 and Dhh1 are involved in the replication of positive-strand RNA viruses by influencing translation and exit from translation to replication of viral RNAs [37–39]. Furthermore, overexpression of Lsm1 and Rck/p54 in human cells has been associated with tumor development [40–43]. The identification of such a central player in RNA fate regulation now opens new options to analyse and manipulate P-body-dependent processes in humans.

## Acknowledgements

We thank the donation of polyclonal anti-Lsm1 antibodies and pYCFPhLSM1 by Reinhard Lührmann, of GFP-DCP1 by Bertrand Séraphin and of pQE30/RCK by Yukihiro Akao. This work was supported by a grant from the Spanish Ministerio de Educación y Ciencia (BFU2004-00654), the German National Genome Research Network (NGFN) and a grant from the Saarland University.

## Appendix A. Supplementary data

Supplementary data associated with this article can be found, in the online version, at doi:10.1016/j.bbamcr.2007.08.009.

## References

- [1] P. Anderson, N. Kedersha, RNA granules, *J. Cell Biol.* 172 (2006) 803–808.
- [2] A. Eulalio, I. Behm-Ansmant, E. Izaurralde, P bodies: at the crossroads of post-transcriptional pathways, *Nat. Rev., Mol. Cell Biol.* 8 (2007) 9–22.
- [3] A. Jakymiw, K.M. Pauley, S. Li, K. Ikeda, S. Lian, T. Eystathiou, M. Satoh, M.J. Fritzler, E.K. Chan, The role of GW/P-bodies in RNA processing and silencing, *J. Cell Sci.* 120 (2007) 1317–1323.
- [4] N. Kedersha, G. Stoecklin, M. Ayodele, P. Yacono, J. Lykke-Andersen, M.J. Fritzler, D. Scheuner, R.J. Kaufman, D.E. Golan, P. Anderson, Stress granules and processing bodies are dynamically linked sites of mRNP remodeling, *J. Cell Biol.* 169 (2005) 871–884.



- [5] R. Parker, U. Sheth, P bodies and the control of mRNA translation and degradation, *Mol. Cell* 25 (2007) 635–646.
- [6] D. Teixeira, U. Sheth, M.A. Valencia-Sanchez, M. Brengues, R. Parker, Processing bodies require RNA for assembly and contain nontranslating mRNAs, *RNA* 11 (2005) 371–382.
- [7] Z. Yang, A. Jakymiw, M.R. Wood, T. Eystathiou, R.L. Rubin, M.J. Fritzler, E.K. Chan, GW182 is critical for the stability of GW bodies expressed during the cell cycle and cell proliferation, *J. Cell Sci.* 117 (2004) 5567–5578.
- [8] J. Collier, R. Parker, Eukaryotic mRNA decapping, *Ann. Rev. Biochem.* 73 (2004) 861–890.
- [9] C. Bonnerot, R. Boeck, B. Lapeyre, The two proteins Pat1p (Mrt1p) and Spb8p interact in vivo, are required for mRNA decay, and are functionally linked to Pab1p, *Mol. Cell. Biol.* 20 (2000) 5939–5946.
- [10] W. He, R. Parker, The yeast cytoplasmic Lsm1/Pat1p complex protects mRNA 3' termini from partial degradation, *Genetics* 158 (2001) 1445–1455.
- [11] S. Zhang, C.J. Williams, K. Hagan, S.W. Peltz, Mutations in VPS16 and MRT1 stabilize mRNAs by activating an inhibitor of the decapping enzyme, *Mol. Cell. Biol.* 19 (1999) 7568–7576.
- [12] J. Collier, R. Parker, General translational repression by activators of mRNA decapping, *Cell* 122 (2005) 875–886.
- [13] F. Wyers, M. Minet, M.E. Dufour, L.T. Vo, F. Lacroute, Deletion of the *PAT1* gene affects translation initiation and suppresses a *PAB1* gene deletion in yeast, *Mol. Cell. Biol.* 20 (2000) 3538–3549.
- [14] S. Tharun, R. Parker, Targeting an mRNA for decapping: displacement of translation factors and association of the Lsm1p-7p complex on deadenylated yeast mRNAs, *Mol. Cell* 8 (2001) 1075–1083.
- [15] R.P. Rother, M.B. Frank, P.S. Thomas, Purification, primary structure, bacterial expression and subcellular distribution of an oocyte-specific protein in *Xenopus*, *Eur. J. Biochem.* 206 (1992) 673–683.
- [16] M.T. Murray, G. Krohne, W.W. Franke, Different forms of soluble cytoplasmic mRNA binding proteins and particles in *Xenopus laevis* oocytes and embryos, *J. Cell Biol.* 112 (1991) 1–11.
- [17] E. Birney, D. Andrews, M. Caccamo, Y. Chen, L. Clarke, G. Coates, T. Cox, F. Cunningham, V. Curwen, T. Cutts, T. Down, R. Durbin, X.M. Fernandez-Suarez, P. Flicek, S. Graf, M. Hammond, J. Herrero, K. Howe, V. Iyer, K. Jekosch, A. Kahari, A. Kasprzyk, D. Keefe, F. Kokocinski, E. Kulesha, D. London, I. Longden, C. Melsopp, P. Meidl, B. Overduin, A. Parker, G. Proctor, A. Prlic, M. Rae, D. Rios, S. Redmond, M. Schuster, I. Sealy, S. Searle, J. Severin, G. Slater, D. Smedley, J. Smith, A. Stabenau, J. Stalker, S. Trevanion, A. Ureta-Vidal, J. Vogel, S. White, C. Woodwark, T.J. Hubbard, *Ensembl, Nucleic Acids Res.* 34 (2006) D556–D561.
- [18] D.L. Wheeler, T. Barrett, D.A. Benson, S.H. Bryant, K. Canese, V. Chetvermin, D.M. Church, M. DiCuccio, R. Edgar, S. Federhen, L.Y. Geer, W. Helmberg, Y. Kapustin, D.L. Kenton, O. Khovayko, D.J. Lipman, T.L. Madden, D.R. Maglott, J. Ostell, K.D. Pruitt, G.D. Schuler, L.M. Schriml, E. Sequeira, S.T. Sherry, K. Sirotkin, A. Souvorov, G. Starchenko, T.O. Suzek, R. Tatusov, T.A. Tatusova, L. Wagner, E. Yaschenko, Database resources of the National Center for Biotechnology Information, *Nucleic Acids Res.* 34 (2006) D173–D180.
- [19] S.F. Altschul, T.L. Madden, A.A. Schaffer, J. Zhang, Z. Zhang, W. Miller, D.J. Lipman, Gapped BLAST and PSI-BLAST: a new generation of protein database search programs, *Nucleic Acids Res.* 25 (1997) 3389–3402.
- [20] K. Katoh, K. Kuma, T. Miyata, H. Toh, Improvement in the accuracy of multiple sequence alignment program MAFFT, *Genome Inform.* 16 (2005) 22–33.
- [21] R. Chenna, H. Sugawara, T. Koike, R. Lopez, T.J. Gibson, D.G. Higgins, J.D. Thompson, Multiple sequence alignment with the Clustal series of programs, *Nucleic Acids Res.* 31 (2003) 3497–3500.
- [22] M. Clamp, J. Cuff, S.M. Searle, G.J. Barton, The Jalview Java alignment editor, *Bioinformatics* 20 (2004) 426–427.
- [23] L.J. McGuffin, K. Bryson, D.T. Jones, The PSIPRED protein structure prediction server, *Bioinformatics* 16 (2000) 404–405.
- [24] M. Kozak, Interpreting cDNA sequences: some insights from studies on translation, *Mamm. Genome* 7 (1996) 563–574.
- [25] N. Cougot, S. Babajko, B. Seraphin, Cytoplasmic foci are sites of mRNA decay in human cells, *J. Cell Biol.* 165 (2004) 31–40.
- [26] D. Ingelfinger, D.J. Arndt-Jovin, R. Luhrmann, T. Achsel, The human LSm1–7 proteins colocalize with the mRNA-degrading enzymes Dcp1/2 and Xrn1 in distinct cytoplasmic foci, *RNA* 8 (2002) 1489–1501.
- [27] Y. Akao, H. Yoshida, K. Matsumoto, T. Matsui, K. Hogetu, N. Tanaka, J. Usukura, A tumour-associated DEAD-box protein, rck/p54 exhibits RNA unwinding activity toward c-myc RNAs in vitro, *Genes Cells* 8 (2003) 671–676.
- [28] J. Sambrook, E.F. Fritsch, T. Maniatis, *Molecular cloning: a laboratory manual, Molecular Cloning: A Laboratory Manual, Vol. 1,2,3*, Cold Spring Harbor Laboratory Press, NY, 1989.
- [29] S. Tharun, W. He, A.E. Mayes, P. Lennertz, J.D. Beggs, R. Parker, Yeast Sm-like proteins function in mRNA decapping and decay, *Nature* 404 (2000) 515–518.
- [30] E. Bouveret, G. Rigaut, A. Shevchenko, M. Wilm, B. Seraphin, A Sm-like protein complex that participates in mRNA degradation, *EMBO J.* 19 (2000) 1661–1671.
- [31] N. Fischer, K. Weis, The DEAD box protein Dhh1 stimulates the decapping enzyme Dcp1, *EMBO J.* 21 (2002) 2788–2797.
- [32] Y. Akao, O. Marukawa, H. Morikawa, K. Nakao, M. Kamei, T. Hachiya, Y. Tsujimoto, The rck/p54 candidate proto-oncogene product is a 54-kilodalton D-E-A-D box protein differentially expressed in human and mouse tissues, *Cancer Res.* 55 (1995) 3444–3449.
- [33] U. Sheth, R. Parker, Decapping and decay of messenger RNA occur in cytoplasmic processing bodies, *Science* 300 (2003) 805–808.
- [34] E. van Dijk, N. Cougot, S. Meyer, S. Babajko, E. Wahle, B. Seraphin, Human Dcp2: a catalytically active mRNA decapping enzyme located in specific cytoplasmic structures, *EMBO J.* 21 (2002) 6915–6924.
- [35] M.A. Andrei, D. Ingelfinger, R. Heintzmann, T. Achsel, R. Rivera-Pomar, R. Luhrmann, A role for eIF4E and eIF4E-transporter in targeting mRNPs to mammalian processing bodies, *RNA* 11 (2005) 717–727.
- [36] C.Y. Chu, T.M. Rana, Translation repression in human cells by microRNA-induced gene silencing requires RCK/p54, *PLoS Biol.* 4 (2006) e210.
- [37] A. Mas, I. Alves-Rodrigues, A. Noueiry, P. Ahlquist, J. Diez, Host deadenylation-dependent mRNA decapping factors are required for a key step in brome mosaic virus RNA replication, *J. Virol.* 80 (2006) 246–251.
- [38] J. Diez, M. Ishikawa, M. Kaido, P. Ahlquist, Identification and characterization of a host protein required for efficient template selection in viral RNA replication, *Proc. Natl. Acad. Sci. U. S. A.* 97 (2000) 3913–3918.
- [39] A.O. Noueiry, J. Diez, S.P. Falk, J. Chen, P. Ahlquist, Yeast Lsm1p-7p/Pat1p deadenylation-dependent mRNA-decapping factors are required for brome mosaic virus genomic RNA translation, *Mol. Cell. Biol.* 23 (2003) 4094–4106.
- [40] M.M. Fraser, P.M. Watson, M.M. Fraig, J.R. Kelley, P.S. Nelson, A.M. Boylan, D.J. Cole, D.K. Watson, CaSm-mediated cellular transformation is associated with altered gene expression and messenger RNA stability, *Cancer Res.* 65 (2005) 6228–6236.
- [41] Y. Nakagawa, H. Morikawa, I. Hirata, M. Shiozaki, A. Matsumoto, K. Maemura, T. Nishikawa, M. Niki, N. Tanigawa, M. Ikegami, K. Katsu, Y. Akao, Overexpression of rck/p54, a DEAD box protein, in human colorectal tumours, *Br. J. Cancer* 80 (1999) 914–917.
- [42] K. Hashimoto, Y. Nakagawa, H. Morikawa, M. Niki, Y. Egashira, I. Hirata, K. Katsu, Y. Akao, Co-overexpression of DEAD box protein rck/p54 and c-myc protein in human colorectal adenomas and the relevance of their expression in cultured cell lines, *Carcinogenesis* 22 (2001) 1965–1970.
- [43] K. Miyaji, Y. Nakagawa, K. Matsumoto, H. Yoshida, H. Morikawa, Y. Hongou, Y. Arisaka, H. Kojima, T. Inoue, I. Hirata, K. Katsu, Y. Akao, Overexpression of a DEAD box/RNA helicase protein, rck/p54, in human hepatocytes from patients with hepatitis C virus-related chronic hepatitis and its implication in hepatocellular carcinogenesis, *J. Viral Hepatitis* 10 (2003) 241–248.